

Bedrosian, P.A., and Frost, C.D., 2022, Geophysical extent of the Wyoming Province, western USA: Insights into ancient subduction and craton stability: GSA Bulletin, <https://doi.org/10.1130/B36417.1>.

Supplemental Material

Supplemental Material 1. A published compilation of U-Pb zircon, monazite, titanite and baddeleyite age determinations of igneous and metamorphic rocks from the WP and adjacent areas. This compilation is provided as both an Excel spreadsheet (B36417_SupMat1.xls) and shapefile (B36417_SupMat1.zip).

Supplemental Material 2. A compilation of published magnetotelluric studies over known suture zones (B36417_SupMat2.xls).

Supplemental Material 3. A report and spreadsheet (B36417_SupMat3.xls) documenting a newly reported U-Pb zircon age on gneiss sample 04SP-QF from the Wind River Range, Wyoming.

Supplemental Material 4. Figures summarizing the data fit of the final 3D resistivity model.

Figure S1. Normalized root-mean-square (nRMS) impedance data misfit at each magnetotelluric site within the survey area. Background color map shows resistivity at 15 km depth. Thick white lines indicate interpreted boundary of the Wyoming Province, as described in the main text; dashed where less certain. Blue, yellow and green lines indicate locations of the Deep Probe (Henstock et al., 1998; Snelson et al., 1998; Gorman et al., 2002), Bighorn Arch (Yeck et al., 2014; Worthington et al., 2016) and CIELO seismic experiments. High misfits are concentrated in areas of dense site coverage where resistivity variations over short length scales cannot be adequately modeled given the 10-km cell size of our inverse model.

Figure S2. Normalized root-mean-square (nRMS) tipper misfit at each magnetotelluric site within the survey area. Background color map shows resistivity at 40 km depth. Linework as described in Figure S1.

Figure S3. Normalized root-mean-square (nRMS) data misfit broken down by (a) site, (b) period, and (c) component. Impedance (Z); vertical magnetic-field transfer function (T). Global nRMS values for the homogeneous start model and final inverse model are 38.27 and 3.96, respectively. Misfits are elevated at short periods, particularly in areas of dense station coverage (Fig. S1) where resistivity varies over short length scales that cannot be captured by the 10-km cell size of our inverse model.

Supplemental Material 3: U-Pb zircon geochronology of quartzofeldspathic gneiss sample 04SP-QF from the southern Wind River Range Gneiss Complex, Wyoming

Report by Carol D. Frost, University of Wyoming

Sample number: 04SP-QF

Location: WGS84 T12 679123 4706618

Collection date: July 20, 2004

Collected by: Carol D. Frost, B. Ronald Frost, Peter Schmitz

Sample 04SP-QF was collected from the Willow Creek drainage north of highway 28 near South Pass, southern Wind River Range. The sample is a strongly foliated biotite-quartzofeldspathic gneiss (Fig. S1). The strike of foliation is 55° with a near vertical dip of 88°SE .

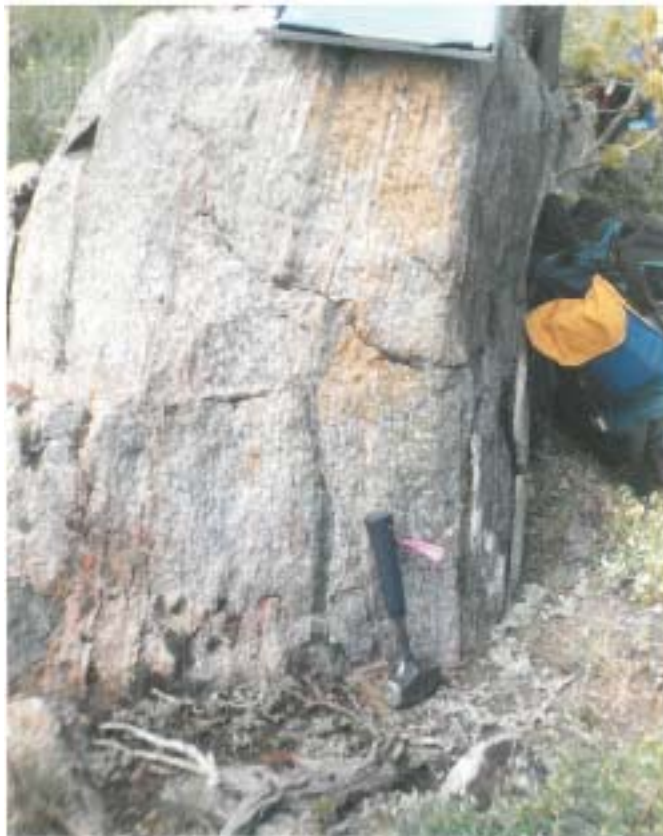


Fig. S1. Field photo of outcrop from which sample 04SP-QF was collected. Hammer for scale.

The sample is part of the Gneiss Complex of Hausel (1991). The Gneiss Complex is intruded by the granodiorite of the Louis Lake batholith to the north and is intercalated with supracrustal rocks of the South Pass greenstone belt on the south. Geochemical analyses of felsic gneiss reported by Hausel (1991) indicate that the felsic gneiss is magnesian, calcic to calc-alkalic, and peraluminous. These compositions lie within the trends defined by the 2.63 Ga Louis Lake batholith on Fe-index, modified alkali-lime index, and aluminum saturation index diagrams. Hausel (1991) interpreted the felsic gneiss as older basement into which the Louis Lake batholith was intruded, and which was tectonically interleaved as thrust slices into the South Pass supracrustal rocks. Our field observations were consistent with this interpretation.

Zircon separation overseen by Kevin Chamberlain. Grains are euhedral, elongate with an aspect ratio of 3:1, and honey to brown in color (Fig. S2). Concentric zoning is apparent in CL. Areas free of cracks or inclusions were selected on 66 grains. These were analyzed by Ian Williams for U-Pb isotopes at the Australian National University on a SHRIMP-RG ion microprobe using methods described by Williams (1998). Analytical data are reported on Table S1.

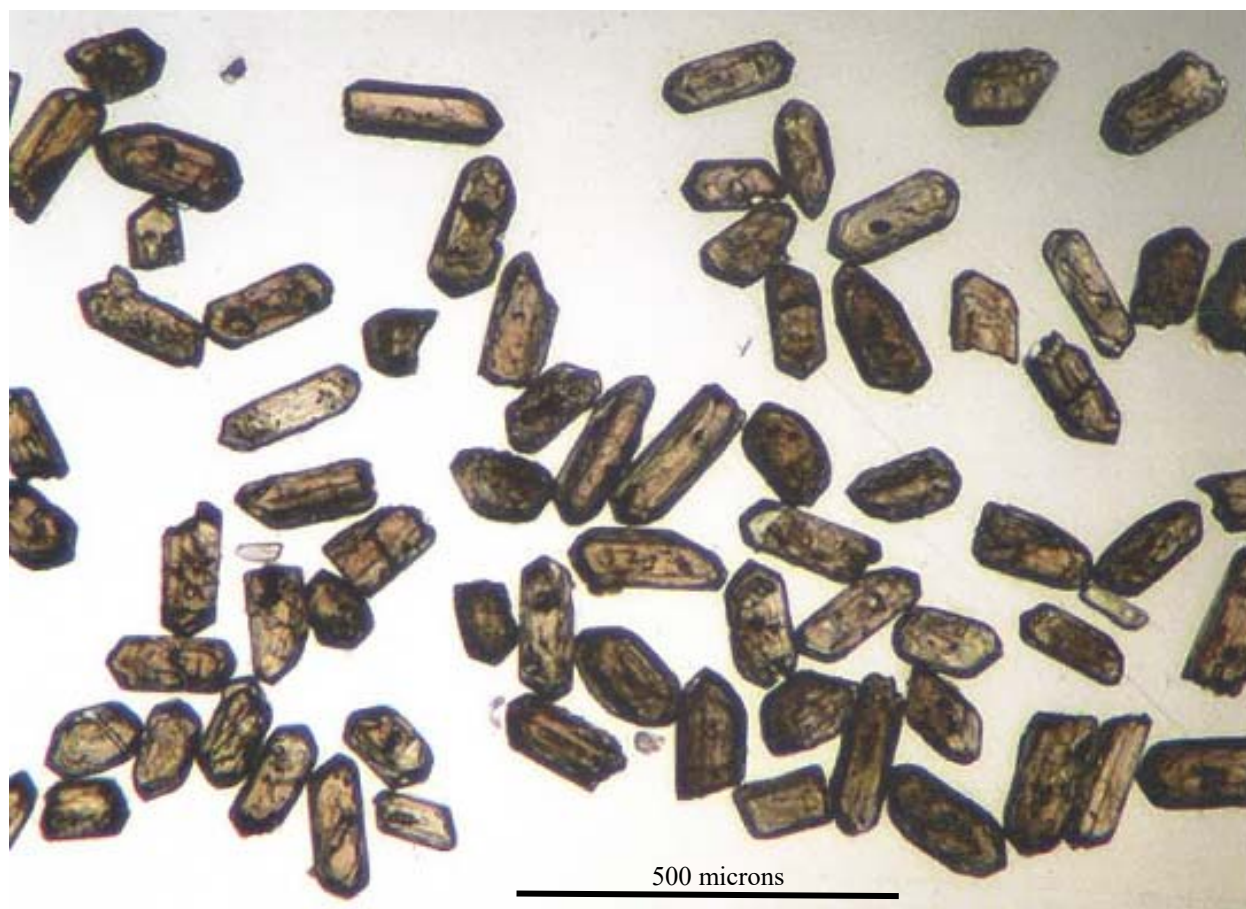


Fig. S2. Representative zircon grains from sample 04SP-QF.

U contents of analyzed areas are high and vary from 300 to over 6000 ppm. Analyses that are positively or strongly negative discordant tend to have high U contents or high ^{204}Pb contents or both. $^{207}\text{Pb}/^{206}\text{Pb}$ ages for 65 of 66 analyzed areas vary from 2882 to 3029 Ma suggesting the sample contains zircon of a single age population. (An additional analysis with much higher analytical uncertainty and strongly reverse discordance gave an older $^{207}\text{Pb}/^{206}\text{Pb}$ age of 3052 ± 46 Ma.) 33 analyses that are up to 10% discordant yield a mean weighted average $^{207}\text{Pb}/^{206}\text{Pb}$ age of 3013.7 ± 1.6 Ma, which is interpreted as the magmatic age of this quartzofeldspathic gneiss (Figure S3).

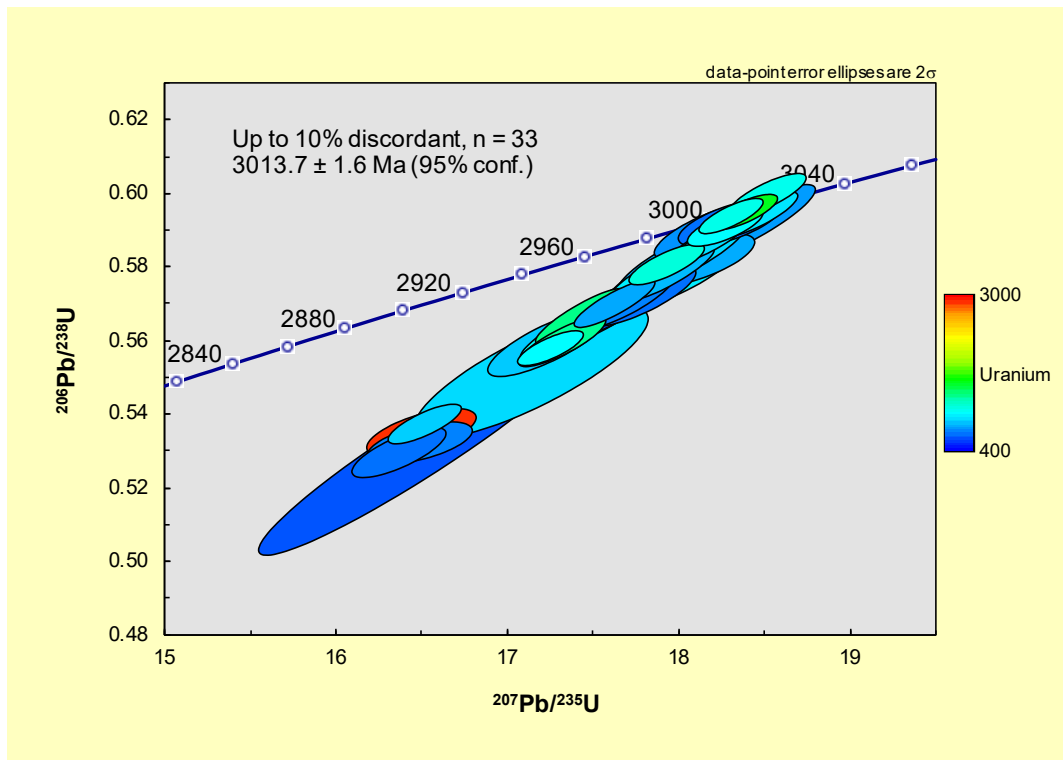


Fig. S3. Concordia plot for 33 analyzed areas of zircon from sample 04SP-QF.

The age of 3014 Ma for this sample confirms the interpretation that the Gneiss Complex of South Pass is basement to the 2.63 Ga Louis Lake batholith. The gneiss is substantially younger than quartzofeldspathic gneiss in the Granite Mountains to the east (3.3–3.45 Ga; Frost et al., 2017). It is similar to the age of the Black Rock Gabbro in the Granite Mountains (3010 ± 1 Ma; Grace et al., 2006), a xenocryst in Bighorn gneiss (3004 ± 17 Ma; Frost and Fanning, 2006) and biotite granite gneiss in the northern Laramie Mountains (3017 ± 11 and 3014 ± 8 Ma; Da Prat, 2020).

REFERENCES CITED

- Da Prat, F.A., 2020, Archean history of the northern Laramie Mountains, M.S. thesis, University of Wyoming, Laramie, Wyoming.
- Frost, C.D., and Fanning, C.M., 2006, Archean geochronological framework of the Bighorn Mountains, Wyoming: *Canadian Journal of Earth Sciences*, v. 43, p. 1399–1418, <https://doi.org/10.1139/e06-051>.
- Frost, C.D., McLaughlin, J.F., Frost, B.R., Fanning, C.M., Swapp, S.M., Kruckenberg, S.C., and Gonzalez, J., 2017, Hadean origins of Paleoproterozoic continental crust in the central Wyoming Province: *Geological Society of America Bulletin*, v. 129, p. 259–280, <https://doi.org/10.1130/B31555.1>.
- Grace, R.L.B., Chamberlain, K.R., Frost, B.R., and Frost, C.D., 2006, Tectonic histories of the Paleo- to Mesoproterozoic Sacawee Block and Neoproterozoic Oregon Trail structural belt of the south-central Wyoming province: *Canadian Journal of Earth Sciences*, v. 43, p. 1445–1466, <https://doi.org/10.1139/e06-083>.
- Hausel, W.D., 1991, Economic geology of the South Pass greenstone belt, southern Wind River Range, western Wyoming: Wyoming State Geological Survey Report of Investigations, no. 44, 129 p.
- Williams, I.S., 1998, U-Th-Pb geochronology by ion microprobe: *Reviews in Economic Geology*, v. v, p. 1–35.

Supplemental Material 4. Figures summarizing the data fit of the final 3D resistivity model.

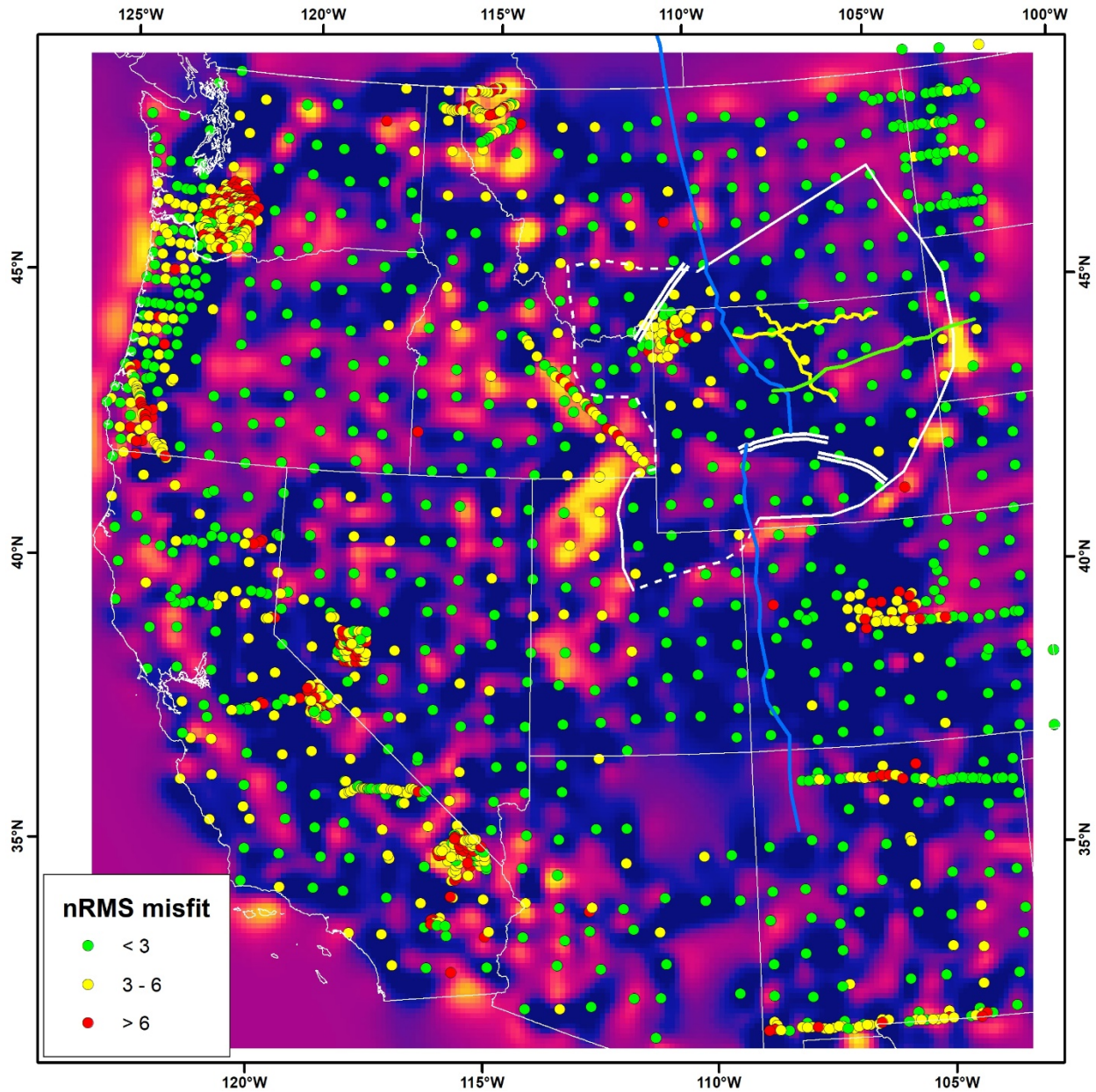


Figure S1. Normalized root-mean-square (nRMS) impedance data misfit at each magnetotelluric site within the survey area. Background color map shows resistivity at 15 km depth. Thick white lines indicate interpreted boundary of the Wyoming Province, as described in the main text; dashed where less certain. Blue, yellow and green lines indicate locations of the Deep Probe (Henstock et al., 1998; Snelson et al., 1998; Gorman et al., 2002), Bighorn Arch (Yeck et al., 2014; Worthington et al., 2016) and CIELO seismic experiments. High misfits are concentrated in areas of dense site coverage where resistivity variations over short length scales cannot be adequately modeled given the 10-km cell size of our inverse model.

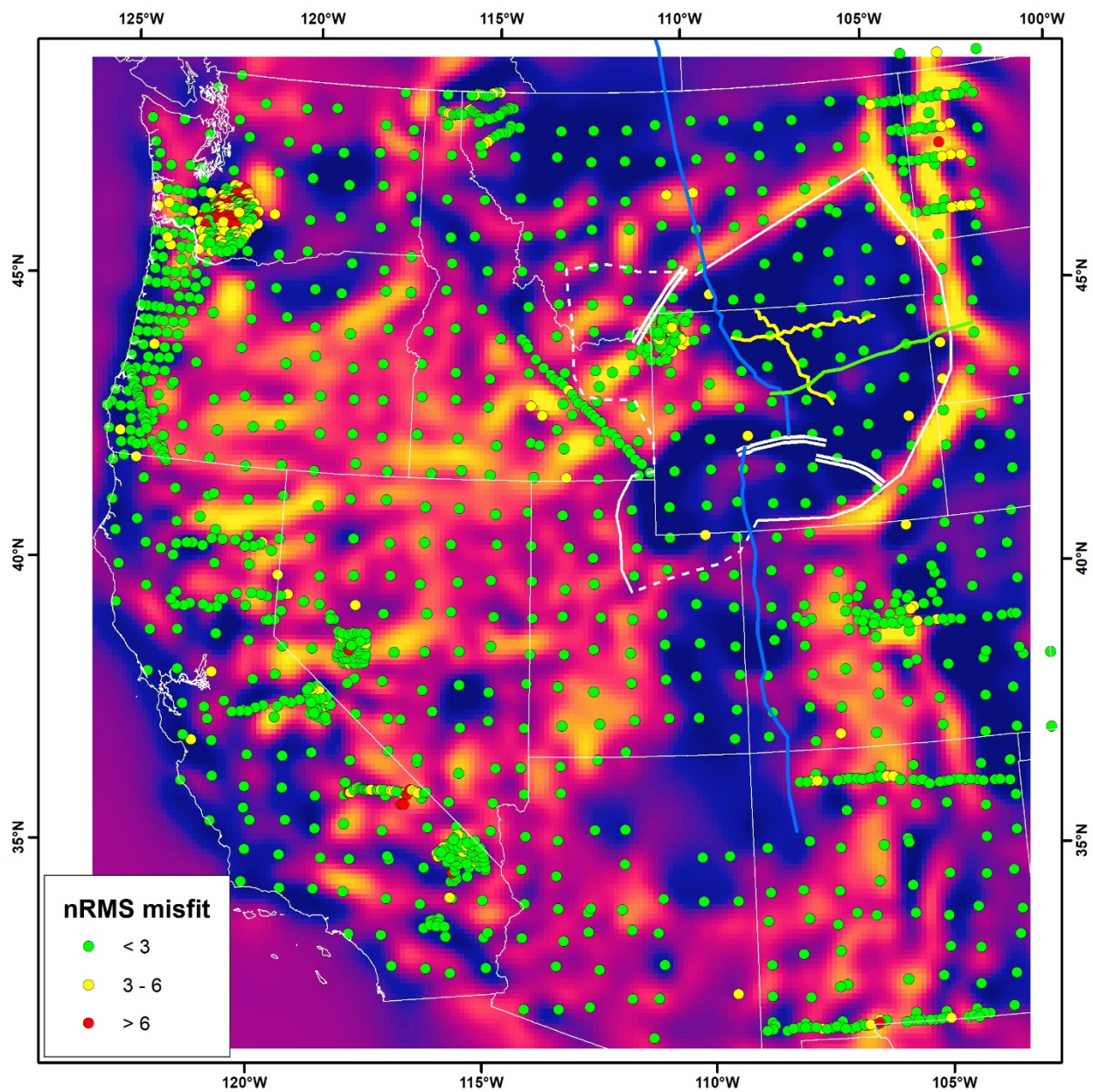


Figure S2. Normalized root-mean-square (nRMS) tipper misfit at each magnetotelluric site within the survey area. Background color map shows resistivity at 40 km depth. Linework as described in Figure S1.

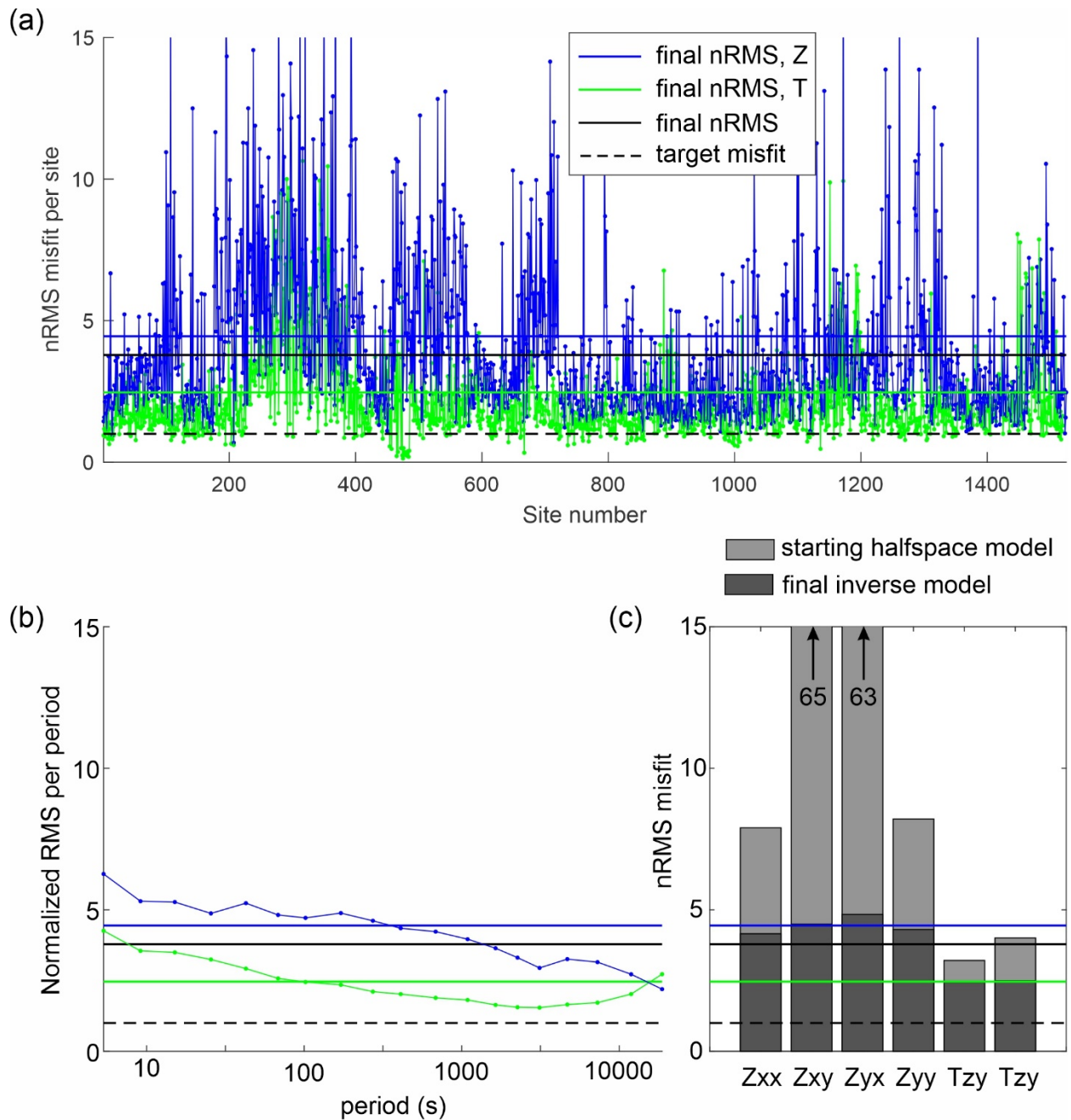


Figure S3. Normalized root-mean-square (nRMS) data misfit broken down by (a) site, (b) period, and (c) component. Impedance (Z); vertical magnetic-field transfer function (T). Global nRMS values for the homogeneous start model and final inverse model are 38.27 and 3.96, respectively. Misfits are elevated at short periods, particularly in areas of dense station coverage (Fig. S1) where resistivity varies over short length scales that cannot be captured by the 10-km cell size of our inverse model.